

RESEARCH ARTICLE | OCTOBER 02 2013

# Assignment of Fermi-level pinning and optical transitions to the $(\text{As}_{\text{Ga}})_2\text{-O}_{\text{As}}$ center in oxygen-doped GaAs

Davide Colleoni; Alfredo Pasquarello



Check for updates

*Appl. Phys. Lett.* 103, 142108 (2013)<https://doi.org/10.1063/1.4824309>View  
OnlineExport  
Citation

## AIP Advances

Why Publish With Us?

**25 DAYS**  
average time  
to 1st decision**740+ DOWNLOADS**  
average per article**INCLUSIVE**  
scope[Learn More](#)

# Assignment of Fermi-level pinning and optical transitions to the $(\text{As}_{\text{Ga}})_2\text{-O}_{\text{As}}$ center in oxygen-doped GaAs

Davide Colleoni<sup>a)</sup> and Alfredo Pasquarello

Chaire de Simulation à l'Echelle Atomique (CSEA), Ecole Polytechnique Fédérale de Lausanne (EPFL),  
CH-1015 Lausanne, Switzerland

(Received 15 August 2013; accepted 20 September 2013; published online 2 October 2013)

The  $(\text{As}_{\text{Ga}})_2\text{-O}_{\text{As}}$  defect in oxygen-doped GaAs, consisting of two As antisites neighboring an O center substitutional to As, is addressed through hybrid functional calculations. This defect not only accounts for the nearest neighbor environment of the O atom and the observed charge states but also yields a Fermi-level pinning position and optical transition energies between charge states in excellent agreement with experiment. The present assignment strongly supports the  $(\text{As}_{\text{Ga}})_2\text{-O}_{\text{As}}$  center as origin of the Fermi-level pinning in oxygen-doped GaAs. © 2013 AIP Publishing LLC. [<http://dx.doi.org/10.1063/1.4824309>]

The widespread use of GaAs semiconductors in technological applications is often hindered by Fermi-level pinning. In several cases, the occurrence of oxygen underlies this behavior.<sup>1–3</sup> In bulk GaAs, oxygen occurs as an unintentional impurity and leads to Fermi-level pinning when present in high concentrations.<sup>1,4,5</sup> A small coverage of oxygen deposited on a GaAs surface is sufficient to pin the Fermi level.<sup>2</sup> Similarly, the major obstacle for realising GaAs-based metal-oxide-semiconductor structures consists in Fermi-level pinning due to the defect density at the GaAs/oxide interface.<sup>3,6</sup> These phenomena lead to different pinning levels and thus apparently result from different mechanisms, but they nevertheless suggest that the development of deeper insight into the origin of Fermi-level pinning in GaAs necessarily goes through the understanding of the role of oxygen.

For the case of oxygen-doped GaAs, a detailed experimental characterization is available.<sup>1,4,5,7–12</sup> The Fermi level has been found to be pinned at 0.4 eV below the conduction band minimum (CBM).<sup>1,5</sup> The study of local vibrational modes (LVM) assigned the origin of this behavior to a Ga-O-Ga center.<sup>1,4,5</sup> Photoexcitation experiments revealed that different charge states are at the origin of three LVM absorption bands, denoted *B*, *B'*, and *A*, at 714.87, 714.21, and 730.65 cm<sup>−1</sup>.<sup>1</sup> It was inferred that the charge states associated to the *A* and *B* bands are stable, while that associated to the *B'* band is metastable.<sup>8,9,12</sup> Magnetic circular dichroism and electron paramagnetic resonance experiments later showed the metastable state to be paramagnetic and to correspond to the neutral charge state.<sup>10,11</sup> The isolated substitutional  $\text{O}_{\text{As}}$  defect was first proposed to explain the experimental features of the Ga-O-Ga center.<sup>7</sup> Semilocal density-functional calculations partially supported this defect model reproducing the Ga-O-Ga structure, the Fermi-level pinning position, and the occurrence of a metastable charge state.<sup>13–15</sup> However, these studies assigned the metastability to the  $-2$  charge state and revealed the occurrence of an additional stable charge state which had not been detected experimentally. Very recently, we showed that the use of a more accurate hybrid functional approach leads to a description of the  $\text{O}_{\text{As}}$  defect which is

inconsistent with the experimental characterization of the Ga-O-Ga center.<sup>16</sup> An alternative model defect showing a Ga-O-Ga unit in its core was proposed by Pesola *et al.* and involved two As antisites neighboring an O center substitutional to As,  $(\text{As}_{\text{Ga}})_2\text{-O}_{\text{As}}$ .<sup>17</sup> This model appears rather complex, but its unoxidized form has recently been invoked for explaining the Fermi-level pinning in highly-damaged GaAs.<sup>18</sup> Semilocal density-functional calculations for the  $(\text{As}_{\text{Ga}})_2\text{-O}_{\text{As}}$  defect gave three different charge states,  $-1$ ,  $0$ , and  $+1$ , and respective vibrational frequencies consistent with the *B*, *B'*, and *A* bands.<sup>17</sup> However, the calculated Fermi-level pinning position differed significantly from the experimental level, thereby preventing a conclusive assignment of the Ga-O-Ga center in oxygen-doped GaAs.

In this work, we aim at identifying the origin of Fermi-level pinning in oxygen-doped GaAs. Using a hybrid functional scheme to obtain accurate defect levels in the band gap, we examine the  $(\text{As}_{\text{Ga}})_2\text{-O}_{\text{As}}$  defect model proposed by Pesola *et al.*<sup>17</sup> In particular, we confront the calculated energy levels of the defect with the Fermi-level pinning position and the optical transition energies as measured in electrical<sup>1,4,5</sup> and photoexcitation experiments,<sup>1</sup> respectively.

The structural relaxations in this work are performed within the generalized gradient approximation proposed by Perdew, Burke, and Ernzerhof (PBE).<sup>19</sup> The electronic properties are then evaluated through the hybrid functional proposed by Heyd, Scuseria, and Ernzerhof (HSE).<sup>20,21</sup> The fraction of nonlocal Fock exchange is set to  $\alpha = 0.35$  in order to reproduce the experimental band gap ( $E_g = 1.52$  eV, Ref. 22), following the approach defined in Ref. 23. We use plane-wave basis sets defined by a kinetic energy cutoff of 70 Ry together with normconserving pseudopotentials. The Brillouin zone is sampled with a  $2 \times 2 \times 2$  mesh which does not contain the  $\Gamma$  point. The exchange potential is treated as described in Ref. 24. We use the Quantum-ESPRESSO suite of programs,<sup>25</sup> with the HSE implementation described in Ref. 26.

The defect is studied through the formation energies of its charge states.<sup>27</sup> We consider the charge states  $-1$ ,  $0$ , and  $+1$ . We adopt As-rich conditions,<sup>28,29</sup> in which the chemical potential of As is set by the  $\text{As}_4$  molecule and that of Ga

<sup>a)</sup>Electronic mail: [davide.colleoni@epfl.ch](mailto:davide.colleoni@epfl.ch)

results from the equilibrium condition in GaAs. The O chemical potential corresponds to the  $O_2$  molecule. The Fermi energies at which the formation energies of different charge states coincide define the charge transition levels. The calculated defect levels critically depend on the position of the GaAs band edges<sup>30–32</sup> and are expected to be accurate within 0.2 eV within the present theoretical scheme.<sup>23</sup> The defect calculations are performed with a 64-atom supercell at the experimental lattice constant of 5.65 Å.<sup>22</sup> To correct for finite-size effects, we use the scheme proposed by Freysoldt, Neugebauer, and Van de Walle.<sup>33</sup> We checked that the potential of the adopted model charge distribution closely reproduces the density-functional potential, indicating that the defect charge is well localized and that the adopted supercell size is adequate.<sup>16,34</sup>

Our relaxed structures of the  $(As_{Ga})_2-O_{As}$  center (Fig. 1) show overall good agreement with those found in Ref. 17. The Ga-O-Ga unit in the defect core is largely insensitive to the charge state with Ga-O bond lengths of  $1.83 \pm 0.01$  Å and a Ga-O-Ga bond angle of  $136.9^\circ \pm 1^\circ$ , thereby accounting for the close frequencies of the LVM bands. The As antisites in the defect core show more significant structural

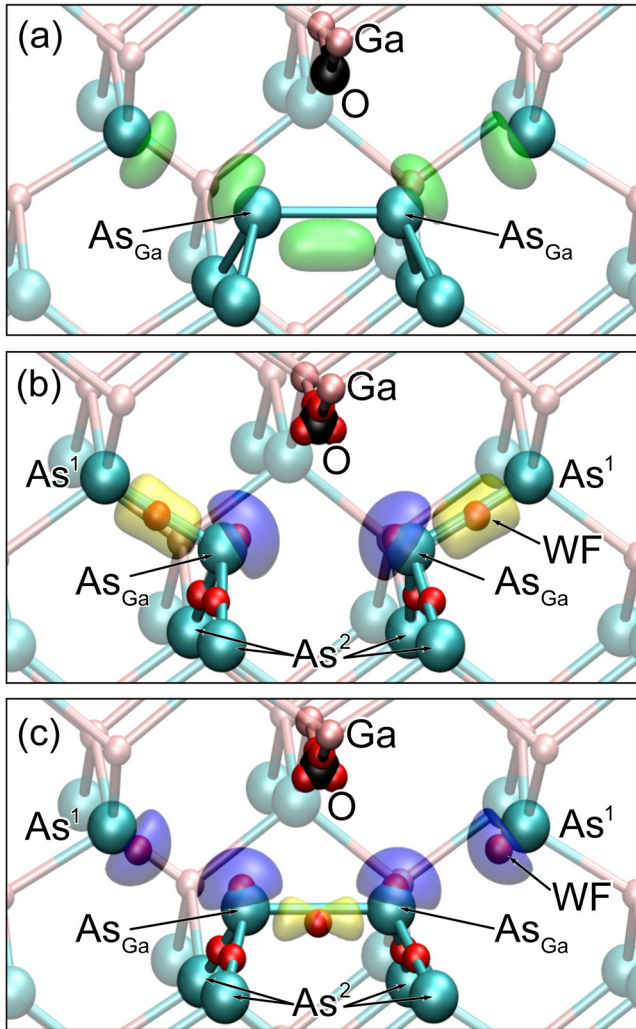


FIG. 1. Relaxed structures of the  $(As_{Ga})_2-O_{As}$  defect in the charge states (a,c)  $-1$  and (b)  $+1$ . In (a), an isosurface of the charge density of the highest occupied orbital is shown. In (b) and (c), relevant maximally localized Wannier functions (WF) are illustrated through their centers (small spheres) and through their isosurfaces.

variations among the charge states. To explain the observed features, we adopt an analysis based on maximally localized Wannier functions (WFs)<sup>35</sup> which allow for a real-space representation of the electron localization. In the positive charge state, the As antisites form three bonds with the surrounding As atoms, as shown in Fig. 1(b). The  $As_{Ga}-As$  distances are  $2.52 \pm 0.01$  Å, while the  $As_{Ga}-As_{Ga}$  distance is 3.52 Å. In our electronic-structure analysis, we find a single WF between the  $As_{Ga}$  and its As neighbors while two such WFs are found in between the As antisites. This indicates that the former linkages correspond to regular bonds, while the central antisites are not bonded and each of them carries a doubly occupied dangling bond (DB) pointing to the Ga-O-Ga unit [Fig. 1(b)]. In the negative charge state, the two As antisites are found at a closer distance of 2.74 Å, while the distances between the central As antisites and their neighboring  $As^1$  increases to 2.89 Å. The WF analysis indicates that the former linkage now corresponds to a regular bond while the latter are no longer bonded and give rise to the appearance of DBs at the  $As^1$  sites [Fig. 1(c)]. The  $As_{Ga}-As^2$  bond length is found to remain almost unchanged, at a value of 2.48 Å. The addition of two electrons to the charge state  $+1$  thus leads to the net effect of transforming one of the As-As bonds into a couple of doubly occupied DBs. The structural variations between the  $+1$  and  $-1$  charge states are at the origin of the negative- $U$  behavior of this center (vide infra). We note that the DBs on the central As antisites in the charge state  $-1$  have slightly turned away from the Ga-O-Ga core structure, thereby lowering the steric constraints on the O vibrational modes and providing a simple explanation for the lower frequency of the  $B$  band with respect to that of the  $A$  band. In the neutral charge state, the  $As_{Ga}-As_{Ga}$  bond is only singly occupied, in agreement with the paramagnetic behavior observed experimentally.<sup>11</sup> Moreover, the depletion of the central  $As_{Ga}-As_{Ga}$  bond leads to a slight increase of the  $As_{Ga}-As_{Ga}$  bond length (2.99 Å) and to a slight decrease of the  $As_{Ga}-As^1$  distance (2.72 Å) as compared with the negative charge state. The DBs of the central As antisites do not change their orientation with respect to the charge  $-1$ , consistent with the close frequencies of the  $B$  and  $B'$  bands.

In III-V materials like GaAs, the electron counting rule is expected to govern the local electronic structure.<sup>16,36</sup> Twofold coordinated O atoms, tetrahedrally bonded Ga, and tetrahedrally bonded As atoms account for  $1$ ,  $\frac{3}{4}$ , and  $\frac{5}{4}$  electrons per bond, respectively. Based on our WF analysis, we find that both the  $+1$  and  $-1$  charge states satisfy the electron counting rule condition. Indeed, these two charge states correspond to stable electronic configurations of the defect (vide infra).

The calculated formation energies of the  $(As_{Ga})_2-O_{As}$  center are shown as a function of Fermi energy in Fig. 2 for As-rich conditions. The  $(As_{Ga})_2-O_{As}$  center is found to be stable in both the charge states  $+1$  and  $-1$ , while the neutral charge state is metastable for all values of the Fermi energy in the band gap in agreement with experimental observations.<sup>10</sup> The defect shows amphoteric behavior acting as an electron donor for low Fermi levels in the band gap and, conversely, as an electron trap for high Fermi levels. This type of defect can lead to Fermi-level pinning at the energy where positive and negative charge states coexist.<sup>37</sup> Overall, the

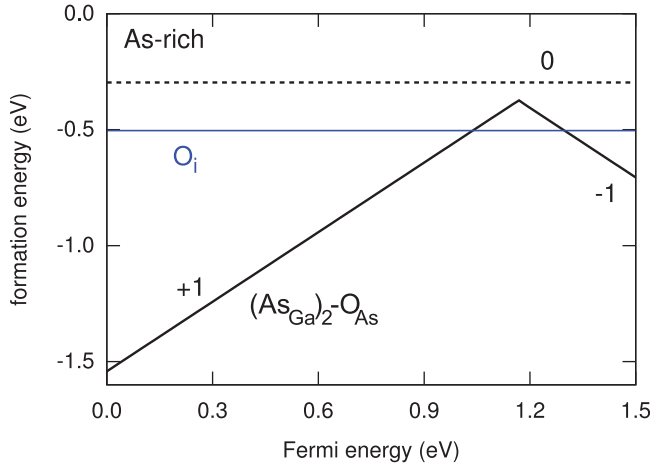


FIG. 2. Formation energies of the  $(\text{As}_{\text{Ga}})_2\text{-O}_{\text{As}}$  defect calculated within HSE in As-rich conditions for the stable charge states +1 and -1 (solid, black) and for the metastable neutral charge state (dashed, black). For comparison, the formation energy of the neutral O interstitial ( $\text{O}_i$ ) bridging a Ga and an As atom is also given (solid, blue). The Fermi energies are referred with respect to the valence band maximum.

hybrid functional calculations are in agreement with the semi-local results of Pesola *et al.*<sup>17</sup> However, the charge transition level  $\varepsilon(+/-)$  in the present calculations occurs at 0.39 eV below the CBM, as a consequence of the opening of the band gap in the hybrid functional description.<sup>23,30</sup> As can be seen from Table I, this brings the level in very close agreement with the experimental Fermi-level pinning position at  $0.40 \pm 0.03$  eV below the CBM.<sup>1,4,5</sup> This result confers strong support to the assignment of the Fermi-level-pinning behavior to the  $(\text{As}_{\text{Ga}})_2\text{-O}_{\text{As}}$  center.

For comparison, we consider the Ga-O-As center which is frequently observed as a distinct defect in LVM experiments.<sup>1,7,38</sup> We model this center by considering the oxygen interstitial ( $\text{O}_i$ ) bridging a Ga and an As atom. As shown in Fig. 2, only the neutral charge state of  $\text{O}_i$  is found to be stable for Fermi energies in the band gap. This result generally agrees with previous semilocal calculations,<sup>13,14</sup> but invalidates the occurrence of negative charge states just below the CBM.<sup>14</sup> The  $(\text{As}_{\text{Ga}})_2\text{-O}_{\text{As}}$  defect is generally more stable than the  $\text{O}_i$  defect, except for a narrow range of Fermi energies around the  $+/-$  charge transition level of the  $(\text{As}_{\text{Ga}})_2\text{-O}_{\text{As}}$  defect, i.e., between 1.0 eV and 1.3 eV above the valence band maximum. In this range, the two defects are competitive and their formation energies differ by at most 0.13 eV, consistent with the fact that the Ga-O-As and Ga-O-Ga centers are simultaneously detected in LVM experiments.<sup>1,7,38</sup> At

TABLE I. Calculated charge transition level  $\varepsilon(+/-)$  referred to the CBM and optical transition energies for the  $(\text{As}_{\text{Ga}})_2\text{-O}_{\text{As}}$  center, compared with experimental results. Energies are given in eV.

	Theory	Experiment
Fermi-level pinning		
$\varepsilon(+/-)$	-0.39	-0.43 <sup>a</sup> , -0.36 <sup>b</sup>
Optical transitions		
$A \rightarrow B'$	1.39	1.37 <sup>a</sup>
$B \rightarrow B'$	0.69	0.65 <sup>a</sup>

<sup>a</sup>Reference 1.

<sup>b</sup>Reference 4.

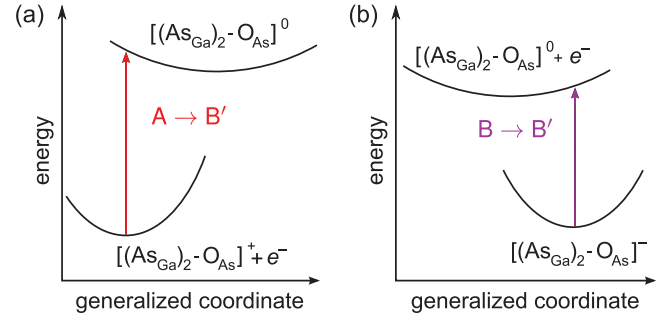


FIG. 3. Schematic configuration-coordinate diagrams illustrating the optical transitions involving the charged states of the  $(\text{As}_{\text{Ga}})_2\text{-O}_{\text{As}}$  defect: (a) from the valence band to the positive charge state of the defect ( $A \rightarrow B'$ ) and (b) from the negative charge state of the defect to the conduction band ( $B \rightarrow B'$ ).

variance, based on the results in Ref. 16, we find that the substitutional  $\text{O}_{\text{As}}$  defect is less stable than the  $(\text{As}_{\text{Ga}})_2\text{-O}_{\text{As}}$  defect by at least 0.47 eV for varying Fermi energy in the band gap. This is also consistent with the absence of any signature pertaining to the  $\text{O}_{\text{As}}$  defect in LVM measurements.<sup>38</sup>

A detailed characterization of the Ga-O-Ga center has been provided in terms of optical transition energies between its charge states,<sup>1</sup> against which the  $(\text{As}_{\text{Ga}})_2\text{-O}_{\text{As}}$  defect model has hitherto not adequately been confronted. Following the experimental work of Alt,<sup>1</sup> we focus on the optical transitions from the valence band to the positive charge state of the defect ( $A \rightarrow B'$ ) and from the negative charge state of the defect to the conduction band ( $B \rightarrow B'$ ). In the corresponding calculations, the optical transition energies are obtained by keeping fixed the structural configuration of the initial state, as illustrated in Fig. 3 through configuration-coordinate diagrams. As given in Table I, calculated and measured transition energies agree within less than 0.05 eV, thereby further corroborating the assignment of the Ga-O-Ga center to the  $(\text{As}_{\text{Ga}})_2\text{-O}_{\text{As}}$  defect.

In conclusion, the  $(\text{As}_{\text{Ga}})_2\text{-O}_{\text{As}}$  defect in oxygen-doped GaAs is addressed through hybrid functional calculations. This defect is found to accurately account for the experimental Fermi-level-pinning position. Furthermore, the optical transition energies between its charge states closely reproduce the experimental values. These results bring the theoretical description of the  $(\text{As}_{\text{Ga}})_2\text{-O}_{\text{As}}$  defect in agreement with the full experimental characterization of the Ga-O-Ga center and strongly support this defect as origin of the Fermi-level pinning in oxygen-doped GaAs.

Financial support is acknowledged from the Swiss National Science Foundation (Grant Nos. 200020-134600 and 206021-128743). We used computational resources of CSCS and CSEA-EPFL.

<sup>1</sup>H. C. Alt, *Phys. Rev. Lett.* **65**, 3421 (1990).

<sup>2</sup>W. E. Spicer, I. Landau, P. Skeath, C. Y. Su, and P. Chye, *Phys. Rev. Lett.* **44**, 420 (1980).

<sup>3</sup>G. Brammertz, H. Lin, K. Martens, A.-R. Alian, C. Merckling, J. Penaud, D. Kohen, W.-E. Wang, S. Sioncke, A. Delabie, M. Meuris, M. R. Caymax, and M. Heyns, *ECS Trans.* **19**, 375 (2009).

<sup>4</sup>H. C. Alt, Y. V. Gomeniuk, and U. Kretzer, *J. Appl. Phys.* **101**, 073516 (2007).

<sup>5</sup>M. Jordan, M. Linde, T. Hangleiter, and J. Spaeth, *Semicond. Sci. Technol.* **7**, 731 (1992).



- <sup>6</sup>M. Caymax, G. Brammertz, A. Delabie, S. Sioncke, D. Lin, M. Scarrozza, G. Pourtois, W.-E. Wang, M. Meuris, and M. Heyns, *Microelectron. Eng.* **86**, 1529 (2009).
- <sup>7</sup>J. Schneider, B. Dischler, H. Seelewind, P. M. Mooney, J. Lagowski, M. Matsui, D. R. Beard, and R. C. Newman, *Appl. Phys. Lett.* **54**, 1442 (1989).
- <sup>8</sup>H. C. Alt, *Appl. Phys. Lett.* **55**, 2736 (1989).
- <sup>9</sup>H. C. Alt, *Appl. Phys. Lett.* **54**, 1445 (1989).
- <sup>10</sup>F. K. Koschnick, M. Linde, M. V. B. Pinheiro, and J.-M. Spaeth, *Phys. Rev. B* **56**, 10221 (1997).
- <sup>11</sup>M. Linde, J.-M. Spaeth, and H. C. Alt, *Appl. Phys. Lett.* **67**, 662 (1995).
- <sup>12</sup>M. Skowronski, S. T. Neild, and R. E. Kremer, *Appl. Phys. Lett.* **57**, 902 (1990).
- <sup>13</sup>T. Mattila and R. M. Nieminen, *Phys. Rev. B* **54**, 16676 (1996).
- <sup>14</sup>W. Orellana and A. C. Ferraz, *Phys. Rev. B* **61**, 5326 (2000).
- <sup>15</sup>R. Jones and S. Öberg, *Phys. Rev. Lett.* **69**, 136 (1992).
- <sup>16</sup>D. Colleoni and A. Pasquarello, "The O<sub>As</sub> defect in GaAs: A hybrid density functional study," *Appl. Surf. Sci.* (published online).
- <sup>17</sup>M. Pesola, J. Boehm, V. Sammalkorpi, T. Mattila, and R. M. Nieminen, *Phys. Rev. B* **60**, R16267 (1999).
- <sup>18</sup>D. Colleoni and A. Pasquarello, *Microelectron. Eng.* **109**, 50 (2013).
- <sup>19</sup>J. P. Perdew, K. Burke, and M. Ernzerhof, *Phys. Rev. Lett.* **77**, 3865 (1996).
- <sup>20</sup>J. Heyd, G. E. Scuseria, and M. Ernzerhof, *J. Chem. Phys.* **118**, 8207 (2003).
- <sup>21</sup>J. Heyd, G. E. Scuseria, and M. Ernzerhof, *J. Chem. Phys.* **124**, 219906 (2006).
- <sup>22</sup>I. Vurgaftman, J. R. Meyer, and L. R. Ram-Mohan, *J. Appl. Phys.* **89**, 5815 (2001).
- <sup>23</sup>H.-P. Komsa and A. Pasquarello, *Phys. Rev. B* **84**, 075207 (2011).
- <sup>24</sup>P. Broqvist, A. Alkauskas, and A. Pasquarello, *Phys. Rev. B* **80**, 085114 (2009).
- <sup>25</sup>P. Giannozzi, S. Baroni, N. Bonini, M. Calandra, R. Car, C. Cavazzoni, D. Ceresoli, G. L. Chiarotti, M. Cococcioni, I. Dabo, A. Dal Corso, S. de Gironcoli, S. Fabris, G. Fratesi, R. Gebauer, U. Gerstmann, C. Gougoussis, A. Kokalj, M. Lazzeri, L. Martin-Samos, N. Marzari, F. Mauri, R. Mazzarello, S. Paolini, A. Pasquarello, L. Paulatto, C. Sbraccia, S. Scandolo, G. Sclauzero, A. P. Seitsonen, A. Smogunov, P. Umari, and R. M. Wentzcovitch, *J. Phys. Condens. Matter* **21**, 395502 (2009).
- <sup>26</sup>H.-P. Komsa, P. Broqvist, and A. Pasquarello, *Phys. Rev. B* **81**, 205118 (2010).
- <sup>27</sup>C. G. Van de Walle and J. Neugebauer, *J. Appl. Phys.* **95**, 3851 (2004).
- <sup>28</sup>P. Rudolph and M. Jurisch, *J. Cryst. Growth* **198**, 325 (1999).
- <sup>29</sup>C. L. Hinkle, M. Milojevic, B. Brennan, A. M. Sonnet, F. S. Aguirre-Tostado, G. J. Hughes, E. M. Vogel, and R. M. Wallace, *Appl. Phys. Lett.* **94**, 162101 (2009).
- <sup>30</sup>A. Alkauskas, P. Broqvist, and A. Pasquarello, *Phys. Rev. Lett.* **101**, 046405 (2008).
- <sup>31</sup>A. Alkauskas, P. Broqvist, and A. Pasquarello, *Phys. Status Solidi B* **248**, 775 (2011).
- <sup>32</sup>A. Alkauskas and A. Pasquarello, *Phys. Rev. B* **84**, 125206 (2011).
- <sup>33</sup>C. Freysoldt, J. Neugebauer, and C. G. Van de Walle, *Phys. Rev. Lett.* **102**, 016402 (2009).
- <sup>34</sup>H.-P. Komsa, T. T. Rantala, and A. Pasquarello, *Phys. Rev. B* **86**, 045112 (2012).
- <sup>35</sup>N. Marzari, A. A. Mostofi, J. R. Yates, I. Souza, and D. Vanderbilt, *Rev. Mod. Phys.* **84**, 1419 (2012).
- <sup>36</sup>J. Robertson and L. Lin, *Appl. Phys. Lett.* **99**, 222906 (2011).
- <sup>37</sup>W. Walukiewicz, *J. Vac. Sci. Technol. B* **5**, 1062 (1987).
- <sup>38</sup>M. Skowronski and R. E. Kremer, *J. Appl. Phys.* **69**, 7825 (1991).